Discrete Linking Transitions For A Superdeformed Band In The $A \approx 80$ Region

C. J. Chiara,[a] D. G. Sarantites,[a] M. Montero,[a] J. O'Brien,[a] O. L. Pechenaya,[a] W. Reviol,[a] R. M. Clark,[b] P. Fallon,[b] A. Görgen,[b] A. O. Macchiavelli,[b] D. Ward,[b] and W. Satuła[c]

[a]*Chemistry Department, Washington University, St. Louis, Missouri 63130 USA*
[b]*Nuclear Science Division, Lawrence Berkeley National Laboratory, Berkeley, California 94720 USA*
[c]*Institute of Theoretical Physics, Warsaw University, Hoża 69, PL-00681, Warsaw, Poland*

Abstract. The yrast superdeformed (SD) band in ^{84}Zr has been linked to states of normal deformation (ND) by three single-step γ decays. The spins and parity of the SD band were determined through angular distributions of two of these links. The properties of this band and its decay to ND states are compared with linked SD bands in other mass regions. SD intensity profiles, calculated SD-ND potential barriers, and results of a statistical-decay analysis suggest there is significant SD-ND mixing involved.

INTRODUCTION

During the past 20 years, over 300 superdeformed (SD) bands have been identified in distinct regions spanning the nuclear chart, but only a fraction of these have been linked by discrete transitions to normal-deformed (ND) states [1]. The observation of links provides additional experimental observables that can be compared with theory, as well as possibly providing insight into the nature of the decay from the SD to ND well. It has been found that links in the light SD regions ($A \approx 40,60$) are often characterized by rather intense decays of stretched $E2$ character, whereas in the heavier SD nuclei ($A \approx 150,190$) the linking transitions typically only carry a few percent of the SD-band intensity and are often of $E1$ character (statistical decays). In the $A \approx 80$ region, although over 30 SD bands in about a dozen nuclei have been identified, none had been linked. The goal of this study was to find linking transitions in the $A \approx 80$ SD region, and compare these results with theoretical predictions and with linked SD bands in other mass regions.

The nucleus ^{84}Zr is a good candidate in which to seek links in this region because, as an even-even nucleus, the lower density of states should provide a simpler decay path to ND states, and the SD states are known to be populated with comparatively high yield in the chosen reaction (see below). In addition, the known SD band in ^{84}Zr has one of the largest deformations in the region, and theoretical calculations predict that SD shell gaps are present at both $Z = 40$ (at large frequencies) and $N = 44$ [2]. Hence, this paper focusses on our recent results for ^{84}Zr.

EXPERIMENTAL DETAILS AND RESULTS

High-spin states in ^{84}Zr were populated via the ^{58}Ni(^{32}S,$\alpha 2p$) reaction. A 140-MeV ^{32}S beam, provided by the 88" cyclotron at Lawrence Berkeley National Laboratory, was directed onto a self-supporting 0.50-mg/cm^2 ^{58}Ni target. The Gammasphere [3] and Microball [4] arrays were used to detect γ rays and charged particles, respectively. Gammasphere consisted of 102 Compton-suppressed HPGe detectors arranged in 16 rings of constant angle θ relative to the beam. A total of 2.2×10^9 events with γ-ray fold five or higher were recorded, along with any correlated Microball pulse-height and timing information. The efficiencies for detecting protons and α particles were $\varepsilon_p \approx 80\%$ and $\varepsilon_\alpha \approx 70\%$, respectively.

CP764, *Nuclei at the Limits,* edited by D. Seweryniak and T. L. Khoo

Events were selected offline that included exactly one α particle and one or two protons. A total of 402×10^6 such events were unfolded into constituent threefold γ coincidences and their energies E_γ incremented into an $E_\gamma - E_\gamma - E_\gamma$ histogram (cube). The $\alpha 3p$ reaction channel was the main contaminant in these particle-gated data; it was considerably reduced in the ($\alpha 2p$+αp)-gated spectra by subtracting normalized $\alpha 3p$-gated spectra following the method given in Ref. [5]. The γ-ray energies were Doppler corrected including an event-by-event correction for the recoil "kicks" provided to the residual nucleus by the emitted particles, as described in Ref. [5]. The RADWARE analysis package [6] was used to project background-subtracted γγ-gated spectra from the cube.

The $\alpha 2p$-gated data were also sorted into $E_\gamma(all) - E_\gamma(\theta)$ histograms (matrices). The $E_\gamma(\theta)$ axis of each matrix was incremented with the energies of γ rays detected in a specific set of Gammasphere rings (similar angles were combined for better statistics); no detection-angle criterion was imposed on the coincident γ rays, which were incremented on the $E_\gamma(all)$ axis. Peak areas and centroids were measured in angle-dependent background-subtracted spectra created by gating on the $E_\gamma(all)$ axis of each matrix and projecting onto the $E_\gamma(\theta)$ axis. Efficiency-corrected intensities of γ rays were obtained as a function of angle from the measured peak areas. Angular correlations were then determined by a least-squares Legendre-polynomial fit of the intensities to the standard expression $W(\theta) = A_0 + A_2P_2(\cos\theta) + A_4P_4(\cos\theta)$ and subsequently used to deduce transition multipolarities.

The peak centroids measured in the ring spectra were used in a residual Doppler-shift lifetime analysis [7]. The residual velocities $<\beta_{res}>$ for an applied recoil velocity β_{app} were deduced from the centroid shifts. The average fractional velocity of the nucleus $<\beta>/\beta_0$ at the time the measured γ ray was emitted is given by the sum of $<\beta_{res}>$ and β_{app}, normalized to the maximum initial velocity β_0. Corrections for a small bias in the measured velocities, resulting from the detection of charged particles with asymmetric efficiency for forward and backward angles, were performed as outlined in Ref. [5].

A partial level scheme of ^{84}Zr, deduced from the coincidence cube, is presented in Fig. 1; only those ND bands relevant to the decay from the SD well are shown (for $I \geq 14\hbar$). These results confirm the decay schemes by Jin *et al*. [8] and Cardona *et al*. [9].

Double gates were placed on pairs of γ rays in band SD1. The spectrum resulting from the sum of all possible double gates in this band is shown on the right side of Fig. 1 (labelled S/S). The three transitions marked with asterisks in this spectrum, at 3464, 3743, and 4052 keV, are candidates for the decay out of the band. Double gating on one of these transitions and the members of band SD1 yields the lower three spectra presented in Fig. 1. In each of these spectra, members of band SD1 are clearly present. In addition, each of the transitions is in coincidence with a different ND structure: 4052 and 3464 keV with positive-parity bands ND1 and ND3, respectively, and 3743 keV with negative-parity band ND2.

Energy sums and coincidence relations are consistent with the placement of the 4052-, 3743-, and 3464-keV γ rays decaying out of the lowest state of band SD1 into the 24^+, 24^-, and (24^+) states of bands ND1, ND2, and ND3, respectively. Thus, these are single-step linking transitions between the SD and ND wells of ^{84}Zr that fix the excitation energies of the states in band SD1.

The intensity of band SD1 (I_{SD1}) is about 3% that of the $2^+ \rightarrow 0^+$ 540-keV transition (not shown). Of this, only about 2% of the I_{SD1} intensity decays through the observed linking transitions, with the 4052-, 3743-, and 3464-keV transitions carrying about 0.9%, 0.7%, and 0.4% of I_{SD1}, respectively. The remaining 98% of the SD1 decay has not been identified in this analysis. Fractions of this intensity are likely carried by transitions that could not be firmly placed in the level scheme, such as the unlabelled peaks in the top spectrum in Fig. 1, or by even weaker (quasicontinuum) transitions.

The multipolarities of the 4052- and 3743-keV linking transitions were obtained through an angular correlation analysis, as described above. The fitted value of A_4/A_0 for the 4052-keV transition was found to be consistent with zero; this parameter was subsequently fixed at zero, resulting in a refitted value for A_2/A_0 of -0.28(7) (which agrees with the result when A_4 is left free). Thus, the angular distribution of this transition is consistent with pure $|\Delta I| = 1$ dipole radiation. The angular distribution of the 3743-keV transition, on the other hand, is *not* peaked at 90° and thus cannot be a pure $|\Delta I| = 1$ dipole. The best-fit values of the A_k coefficients are $A_2/A_0 = 0.27(18)$ and $A_4/A_0 = 0.34(31)$. The uncertainties for these results are too large to make an unambiguous multipolarity assignment, but these values are consistent with a mixed $|\Delta I| = 1$ $M1/E2$ assignment for this transition.

The two bands into which these linking transitions feed, bands ND1 and ND2, have opposite parities. Thus, an $M1/E2$ assignment for the 3743-keV transition implies an $E1$ assignment for the 4052-keV transition. Although these results do not distinguish between $\Delta I = \pm 1$ transitions, it is common to see decays from a nonyrast state to a lower-spin yrast or near-yrast state; hence, the preferred assignment for the lowest observed state in band SD1 is $I^\pi = 25^-$, giving band SD1 odd spins and negative parity.

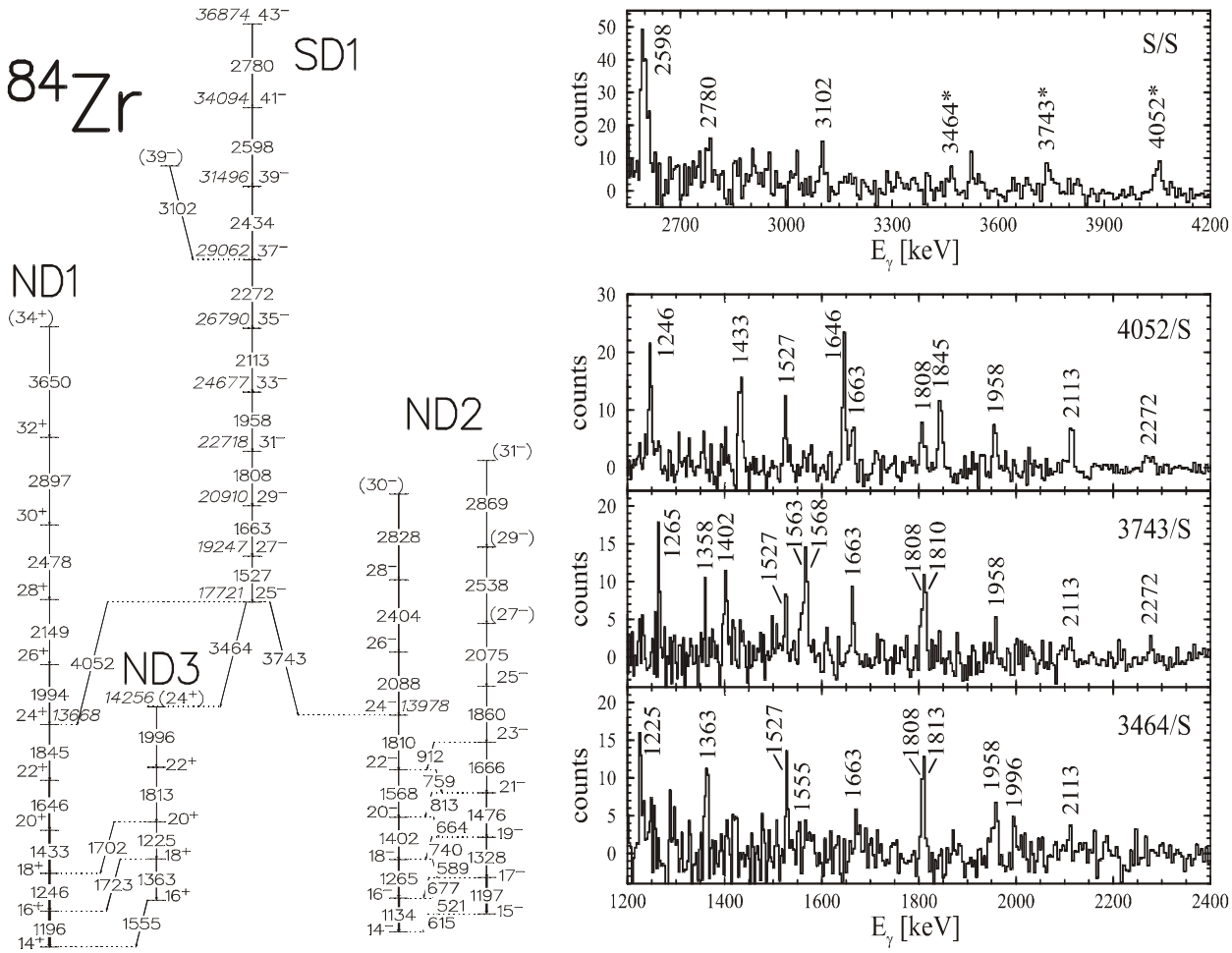

FIGURE 1. Left: Partial level scheme of ^{84}Zr. Energies of states (in italics) and transitions are given in keV. Tentative spin assignments are given in parentheses. Right: Background-subtracted γ-ray energy spectra created from double gates on the transitions indicated on each panel, where S is the set of all γ rays in band SD1. Peaks are labelled with their energies in keV; those marked with an asterisk in the top panel are identified linking transitions.

We determined the lifetime of the 25^- state in band SD1 as follows: First, we measured the $\langle\beta\rangle/\beta_0$ values for the in-band transitions in order to establish the effective lifetime of the feeding into the 25^- state. A fixed Q_t value was assumed for the entire band. The best-fit value of $Q_t = 4.98\pm0.07^{+0.24}_{-0.29}$ eb was obtained through a χ^2 fit using a program developed by Lee [10]. (The method is described in more detail in, e.g., Ref. [11].) The first quoted error is statistical, while the latter is an estimated systematic error due to uncertainties in the target thickness, stopping powers, size of the bias, and side-feeding assumptions. This result is consistent with the value of $Q_t = 5.6^{+0.6}_{-0.5}$ eb presented in Ref. [2].

We then obtained the average $\langle\beta\rangle/\beta_0$ for the 25^- state by summing spectra gated on the in-band SD1 γ rays and fitting the centroid shifts for the 4052-keV γ ray. The lifetime of this state was determined by allowing a "Q_t" value for decay out of this state to vary independently of the rest of the band. (Note that, in this case, "Q_t" is just a fittable parameter from which a lifetime is obtained.) Since gating was from above the state of interest, the effects of any possible side feeding into this state are circumvented. Using this method, a lifetime of $\tau = 20^{+58}_{-14}$ fs was obtained for the 25^- state. The uncertainties may be large, but this measurement at least establishes the lifetime of this state to within an order of magnitude.

The partial lifetimes τ_γ of the linking transitions were obtained from their branching fractions and the lifetime of the 25^- state. The lifetime of the 4052-keV transition corresponds to a reduced transition strength of $B(E1) = (6.4^{+12.9}_{-4.8})\times10^{-6}$ e^{2}fm^2 = $(5.2^{+10.4}_{-3.9})\times10^{-6}$ W.u. The 3464-keV $E1$ was found to have similar strength. For the mixed-

$M1/E2$ 3743-keV γ ray, $B(M1) < 3.3\times10^{-4}$ W.u. (Note that this is an upper limit since the amount of $E2$ admixture is unknown.)

DISCUSSION

The determination of the spins, parities, excitation energies, and average Q_t moment within band SD1, and the decay rates out of the band, makes ^{84}Zr one of the limited number of cases where an SD band has been thus fully characterized. This information permits direct comparison with theoretical predictions. In Ref. [2], Cranked-Strutinsky calculations using the Lipkin-Nogami pairing formalism (CSLN) were performed in a comprehensive study of $A \approx 80$ SD bands. Band SD1 in ^{84}Zr was assigned a configuration having two neutrons and one proton occupying $h_{11/2}$ intruder orbitals ($\nu5^2\pi5^1$). The results of the current analysis agree with the negative-parity assignment given in Ref. [2]. However, the spins are measured to be $4\hbar$ higher than the previous estimate.

For the current study, the CSLN calculations were extended from those of Ref. [2] by using a finer mesh for the $\beta_2 - \gamma$ deformation space and by including more of the ND range of these deformation parameters. The energies and spins for bands SD1 and ND1 are in reasonable agreement with the predictions for the $\nu5^2\pi5^1$ and vacuum configurations, respectively. These results will be discussed in detail in Ref. [12].

We can now compare this linked SD band in ^{84}Zr with examples in other mass regions. Specifically, this band bears similarities to SD bands in the $A \approx 150,190$ regions, where the intensities of the links are also rather small, carrying less than 1% of the SD-band intensity. The weak transitions in several heavy SD nuclei have been previously interpreted in the context of statistical decays. This is in contrast to the links observed in the $A \approx 40$ region and for many cases in the $A \approx 60$ region, which are dominated by rather intense $E2$ decays (see e.g. Ref. [11]). In Fig. 2, partial level schemes of the yrast SD bands in ^{84}Zr, ^{152}Dy [13], and ^{192}Pb [14] show the lowest several SD transitions and their links to ND states for each nucleus. The decay-out spins and excitation energies above yrast for the SD bands in ^{84}Zr and ^{152}Dy are found to be comparable, while the spins (and also, in most cases, the excitation energies) in the $A \approx 190$ region are lower. The $E1$ transition rates in both ^{84}Zr and ^{152}Dy were found to be on the order of $B(E1) \sim 10^{-6}$ W.u., about 10-100 times larger than in the $A \approx 190$ region [14-16]. So in many respects, band SD1 in ^{84}Zr is very similar to the yrast SD band in ^{152}Dy. One noteworthy distinction is that in ^{84}Zr there are no SD transitions observed decaying in parallel to the linking transitions; the relevance of this finding to the analysis will be addressed below.

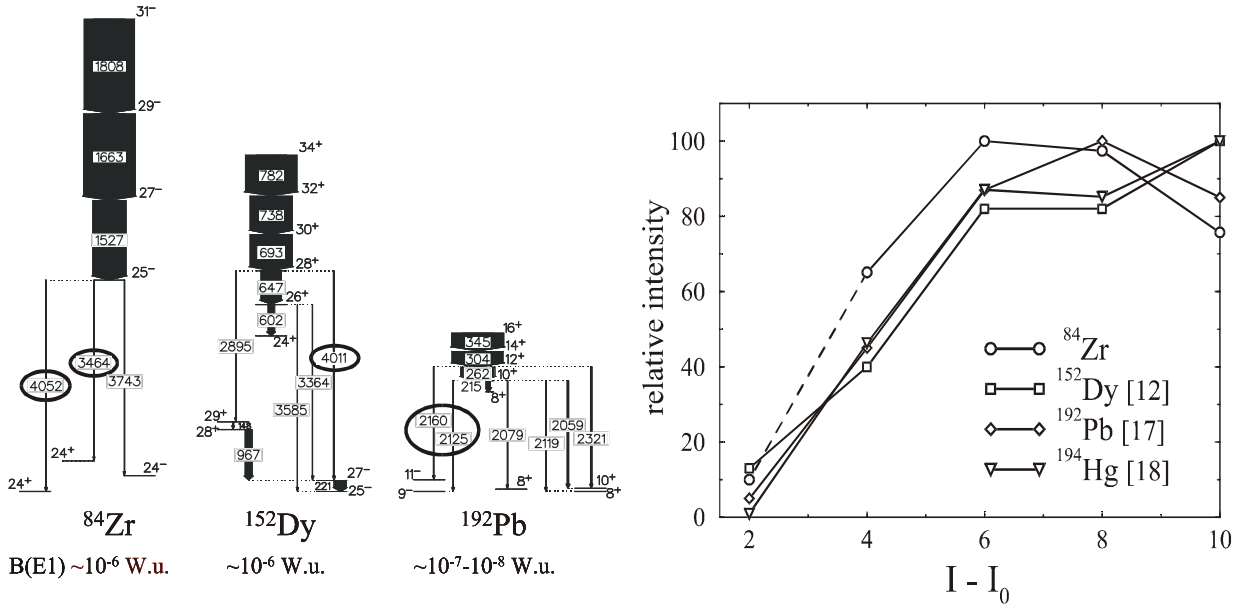

FIGURE 2. Left: Partial level schemes showing the observed decays out of the SD wells in ^{84}Zr, ^{152}Dy, and ^{192}Pb. $B(E1)$ strengths are given for links in each mass region, such as the $E1$ transitions with encircled labels. Right: Intensity profiles for several yrast SD bands. Intensity is normalized to the maximum in the band. Spins are relative to the lowest observed SD state. The lowest point for ^{84}Zr has been estimated (see text).

The intensity profile for typical SD bands features a rapid fall-off below the spin range over which the intensity peaks or plateaus. In ^{84}Zr SD1, there is only one observed γ ray (1527 keV) below the peak in the intensity profile. A second γ ray would likely need to have less than 10% of the band intensity for it to have been unobserved in this analysis. This is in contrast with ^{152}Dy and several other heavy SD nuclei where there are three or four transitions below the peak intensity, as shown on the right in Fig. 2. In other words, the decay out of the SD band in ^{84}Zr proceeds even more rapidly (over fewer states) than in the other nuclei.

The very rapid depopulation of the SD band may be explained by the spin-dependent behavior of the height of the barrier separating the SD and ND wells. In Ref. [19], potential-energy surfaces as a function of fixed spin were calculated for the nuclides ^{152}Dy, ^{143}Eu, and ^{192}Hg. The height of the potential barrier relative to the SD minimum was determined at several spins for each nuclide. For comparison, we extracted values for ^{84}Zr from similar calculations. (These surfaces were calculated as a function of frequency, and the spins were estimated.) *Preliminary* results indicate that the height of the barrier in ^{84}Zr changes more dramatically with spin than do the other examples. At $I \sim 25\hbar$ (the decay-out spin), the barrier height for ^{84}Zr is comparable to the calculated values near the decay-out spins for ^{152}Dy (also $I \sim 25\hbar$) and for the $A \approx 190$ region ($I \sim 10\hbar$). Below this spin, it continues to decrease rapidly. This is consistent with the observed abrupt depopulation of the SD well in ^{84}Zr at a faster rate than in the heavier SD nuclei.

Several models for statistical SD decay have been developed in recent years (see e.g. Refs. [20] and [21], and references therein). In these models, the decay proceeds via the coupling of an SD state to one or more ND states, with the coupling strength related to the ND and SD decay widths (Γ_N and Γ_S), the spreading width $\Gamma^{\downarrow}$ that determines the mixing between ND and SD states, and the average separation d between ND states. Comparisons of the spreading widths and coupling strengths extracted from the $A \approx 150$ and 190 SD data are found to be rather sensitive to the choice of model, differing by orders of magnitude in some cases. On the other hand, there is some consistency in that the different models predict similar relative values for the coupling strengths in the examined nuclei (see Table I in [22]).

Unlike the linked SD bands in the $A \approx 150$ and 190 mass regions, in ^{84}Zr there are no observed in-band SD1 transitions competing with the links to ND states. This introduces uncertainty in a statistical-decay analysis, as only an upper limit on Γ_S can be deduced based on an estimated intensity upper limit for a transition with $E_\gamma \sim 1.37$ MeV (extrapolating the SD1 energies to lower spins). As a starting point for a quantitative comparison, however, we employ the formalism of Ref. [20] in which the in-band SD intensity F_S is expressed as a function of the ratios $\Gamma^{\downarrow}/\Gamma_S$ and Γ_N/d. Using the same expressions for Γ_N and $d = 1/\rho$ (where ρ is the Fermi gas model level density) as in Ref. [22], a lower limit of $\Gamma^{\downarrow}/\Gamma_S > 4.4\times10^6$ is obtained for (a likely overestimated) $F_S < 0.2$. Without quantitative information about the SD decay width, no value can be assigned to $\Gamma^{\downarrow}$ since the limit for the ratio can be satisfied by a sufficiently small value of Γ_S. However, this ratio is up to four orders of magnitude larger than the corresponding ratios for the tabulated values from Ref. [22] (e.g., $\Gamma^{\downarrow}_{GW}/\Gamma_S = 600$ in ^{152}Dy, which is otherwise quite similar to ^{84}Zr), suggesting that mixing between states separated by the potential barrier may be more significant in ^{84}Zr than in the heavier SD regions (except possibly the 10^+ state in ^{192}Pb). This also supports the interpretation that ^{84}Zr may have a smaller barrier between the SD and ND wells near the decay-out spin.

CONCLUSION

In summary, we have identified three discrete transitions in ^{84}Zr that link states in the SD and ND wells by single-step decays. This is the first observation of links in the $A \approx 80$ region of SD. The spins and parity of the linked band were established through the angular distributions of two of the linking transitions. Several properties of the linked band are reasonably well reproduced by Cranked-Strutinsky calculations. The energy above yrast, decay-out spin, and $B(E1)$ decay-out strength for band SD1 in ^{84}Zr are all quite similar to those of the yrast SD band in ^{152}Dy. However, the very abrupt depopulation of this SD band, the estimated $\Gamma^{\downarrow}/\Gamma_S$ ratio, and the (preliminary) calculated potential barrier separating the SD and ND wells all point to a greater mixing of SD and ND states in ^{84}Zr than in the heavier SD nuclei.

ACKNOWLEDGMENTS

We would like to thank A. N. Wilson and R. J. Charity for helpful discussions. This work was supported in part by the U.S. Department of Energy under Grant No. DE-FG02-88ER-40406 and Contract No. DE-AC03-76SF00098, and the Polish Committee for Scientific Research, Contract No. 1 P03B 059 27.

REFERENCES

1. B. Singh, R. Zywina, and R. B. Firestone, Nucl. Data Sheets **97**, 241 (2002).
2. F. Lerma *et al.*, Phys. Rev. C **67**, 044310 (2003).
3. I. Y. Lee, Nucl. Phys. **A520**, 641c (1990).
4. D. G. Sarantites *et al*., Nucl. Instrum. Methods Phys. Res., Sect. A **381**, 418 (1996).
5. C. J. Chiara, D. R. LaFosse, D. G. Sarantites, M. Devlin, F. Lerma, and W. Reviol, Nucl. Instrum. Methods Phys. Res., Sect. A **523**, 374 (2004).
6. D. C. Radford, Nucl. Instrum. Methods Phys. Res., Sect. A **361**, 297 (1995).
7. B. Cederwall *et al.*, Nucl. Instrum. Methods Phys. Res., Sect. A **354**, 591 (1995).
8. H.-Q. Jin *et al.*, Phys. Rev. Lett. **75**, 1471 (1995).
9. R. Cardona *et al.*, Phys. Rev. C **68**, 024303 (2003).
10. I. Y. Lee (private communication).
11. C. J. Chiara *et al.*, Phys. Rev. C **67**, 041303(R) (2003).
12. C. J. Chiara *et al.* (to be submitted).
13. T. Lauritsen *et al.*, Phys. Rev. Lett. **88**, 042501 (2002).
14. A. N. Wilson *et al.*, Phys. Rev. Lett. **90**, 142501 (2003).
15. T. L. Khoo *et al.*, Phys. Rev. Lett. **76**, 1583 (1996).
16. R. Krücken *et al.*, Phys. Rev. C **55**, R1625 (1997).
17. D. P. McNabb *et al.*, Phys. Rev. C **56**, 2474 (1997).
18. G. Hackman *et al.*, Phys. Rev. Lett. **79**, 4100 (1997).
19. K. Yoshida, M. Matsuo, and Y. R. Shimizu, Nucl. Phys. **A696**, 85 (2001).
20. Jian-zhong Gu and H. A. Weidenmüller, Nucl. Phys. **A660**, 197 (1999).
21. D. M. Cardamone, C. A. Stafford, and B. R. Barrett, Phys. Rev. Lett. **91**, 102502 (2003).
22. A. N. Wilson, in Proceedings of the Fusion03 International Conference, Matsushima, Japan, 2003 (to be published in Prog. Theor. Phys.).